KSCE Journal of Civil Engineering (2021) 25(8):3008-3018
DOI 10.1007/s12205-021-1531-6

pISSN 1226-7988, eISSN 1976-3808
www.springer.com/12205

Structural Engineering

A PSO-ANN Intelligent Hybrid Model to Predict the Compressive Strength of Limestone Fillers Roller Compacted Concrete (RCC) to Build Dams

Youcef Chakali[a], **Ahmed Hadj Sadok**[a], **Mahfoud Tahlaiti**[b], **and Tarek Nacer**[a]

[a]*Laboratoire Mobilisation et Valorisation des Ressources en Eau (MVRE), Ecole Nationale Supérieure d'Hydraulique (ENSH), Soumaâ 09000, Algeria*
[b]*Institut Catholique d'Arts et Métiers (ICAM), Nantes 44470, France*

ARTICLE HISTORY

Received 26 August 2020
Revised 15 February 2021
Accepted 15 March 2021
Published Online 24 May 2021

KEYWORDS

Roller compacted concrete
Dam
Limestone fillers
Prediction
Compressive strength
Artificial neural network
Particles swarm optimization

ABSTRACT

The compressive strength of the roller-compacted concrete (RCC) is an essential indicator of quality when designing dams. RCC is optimized in most cases through experimental studies conducted vigorously. This study aims at developing a smart system to predict the compressive strength of the limestone fillers RCC that is used to build dams. The prediction is made base on the following parameters: the maximum diameter of the aggregates, the compactness of the granular mixture, the rates of both cement and limestone fillers, water/cement ratio and the RCC age. The cement strength is taken in to consideration using a corrective equation. Two metaheuristic systems are developed: artificial neural networks (ANN), and a hybrid system consisting of an ANN optimized by a particle swarm optimization (PSO) algorithm. An experimental database is built containing 500 vectors taken from RCC formulations given by lab activity reports about 04 dam projects. The best results were achieved through the PSO-ANN hybrid system. This prediction system is validated by an experimental study conducted on 20 RCC formulations, and a comparison was made with the Laboratoire Central des Ponts et Chaussees (LCPC) method. The prediction resulting from the PSO-ANN system is of a good accuracy level with a correlation factor $R^2 = 0.85$ and a low root mean squared error of 1.45. Finally, a user interface based on the model developed is created.

1. Introduction

In recent years, roller compacted concrete (RCC) has been increasingly used in the construction of dams and pavements because it is technically advantageous and low-cost (Chhorn et al., 2018). Indeed, it offers a fast preparation and longer service life compared to the conventional concrete (Calis and Yıldızel, 2019). RCC dams, which are made with a granular mixture of sand and gravel of various sizes up to 100 mm in diameter, are also characterized by a low cement content to minimize the thermal shrinkage cracking, which represent a huge problem for the durability of dams (Zhang et al., 2020). Fillers are added to increase the compactness of the granular mixture, which can be either pozzolanic or inert such as limestone fillers, being widely used as a result of their availability. In Algeria, there are more than 1,000 limestone aggregate production units, with a total capacity of about 68 million tons annually (Kitouni and Houari, 2013). This production generates a huge amount of fillers causing environmental damage. Besides the environmental benefit of using this material as a concrete addition, its incorporation results in significant improvements in the physical and mechanical properties of concrete, especially RCC (de Larrard, 1999b; Caré et al., 2000; Cyr et al., 2006; Michel et al., 2007). An experimental study showed the improvement of mechanical properties and durability of RCC mixes when cement was substituted by 15% of ground limestone (Yildizel et al., 2020).

The mechanical strength of the RCC remains a parameter of great importance when designing dams. It is used to meet the requirements of structural calculations and as a good indicator of resistance and durability (ACI Committee 207, 1999; Godoi et al., 2019; Sukontasukkul et al., 2019). Therefore, the engineer often needs an effective tool to predict the compressive strength "Fc" for two reasons: predicting "Fc" for the purpose of making structural calculations as well as using the prediction model as an optimization tool in studying the formulation of the RCC itself. The compressive strength of RCC depends on many important

CORRESPONDENCE Mahfoud Tahlaiti mahfoud.tahlaiti@icam.fr Institut Catholique d'Arts et Métiers (ICAM), Nantes 44470, France

parameters: the water rate, the cement rate, the type and properties of fillers and finally aggregate quality. However, the influence of cement rate "Dc" and the water/cement "W/C" ratio remain among the most significant parameters (de Larrard, 1999a). Rahmani et al. (2020b) showed in their experimental study that the variation of the "W/C" ratio (from 0.55 to 0.3) and the cement rate (from 12 to 17%) influence significantly the VEBE time of RCC. This study also showed that the increase of the cement rate, according to the decrease of the "W/C" ratio improves the physical and mechanical properties of the pavement RCC. The same authors, in another experimental study carried out on different RCC mixes, proved the important influence of the W/C ratio variation on the flexural, tensile and compressive strengths and also on the modulus of elasticity of RCC (Rahmani et al., 2020a).

As for the conventional concrete, several models are available for to predict the "Fc", such as the ACI (ACI Committee 209.2R-08, 2008) and CEB (International Federation for Structural Concrete, 2010). In contrast, only few models to predict mechanical strength of RCC have been developed. It is worth noting that many methods of formulation are used to optimize the mechanical strength of RCC. These processes are often based on huge experimental programs with a large number of trial mixes varying the different parameters of influence (Gautier and Marchand, 2017). The report issued by the ACI Committee on dam RCC (ACI Committee 207, 1999), suggests some empirical links showing the variation of "Fc" varies according to C and the W/C ratio for some types of aggregates, while there is no mention of a global prediction model involving a set of parameters impacting resistance. Other effective methods are based on more theoretical approaches, using empirical formulas or well-established theoretical models, but involving a restrictive experimental characterization of the different RCC materials. In this context, the method developed by LCPC (Laboratoire Central des ponts et chausses "Central Laboratory for Roads and Bridges") (de Larrard, 1999a) proposes the prediction of "Fc" by taking into account a very wide range of parameters. This model was developed for the use of conventional concretes but can be adapted to the use of RCC relying on several hypotheses and a many tests in the lab (de Larrard and Sedran, 2009). In this approach, the mineral additions are considered as fillers with a proposed correction depending on the pozzolanic activity. Traditional methods of formulation are money and time consuming, therefore the use of numerical methods of prediction is necessary.

Currently, the use of artificial intelligence has developed in various fields of research in mechanical (Sankar et al., 2019), medicine (Belić et al., 2019) and civil engineering (Tan et al., 2019). Artificial neural networks (ANN), based on human brain functioning, are among the most developed and widely used for prediction and optimization problems (Elsheikh et al., 2019). An ANN is composed of a set of elements (Artificial Neurons), linked by weighted links (weight and bias). The neurons are adjusted in the learning phase to create a model that faithfully reproduces the results of a physical experience. ANN are used to solve problems in several fields, including civil engineering (Yeh, 2006). In fact, neural networks are widely used in the prediction of several parameters of concrete such as workability (Bai et al., 2003), compressive strength (Hammoudi et al., 2019), parameters of formulation (Amlashi et al., 2019) and even the degree of hydration of the cement paste (Park et al., 2005). Recently, artificial intelligence algorithms "metaheuristics" such as genetic algorithms (GA), ant colonies (ACO) or particle swarm optimization algorithms (PSO) are increasingly used for the optimization of ANN neural network parameters. These kinds of algorithms combination lead to develop of hybrid models. These metaheuristics are known for their ability to minimize the time of computation (Boussaid, 2014). PSO algorithms are very successful in various engineering applications (Gopalakrishnan, 2013). Recent papers in the literature proposed hybrid ANN models to predict some physical properties and strength parameters (Qi et al., 2018). Compared to conventional Back-Propagation Neural Networks BP-ANN, the hybrid evolutionary algorithm-based ANN models are more accurate due to their ability to overcome the slow rate of learning and local minima problems (Momeni et al., 2015). Several evolutionary algorithms have been used to enhance the performance of ANN-based predictive models such as genetic algorithms (GA), particle swarm optimization (PSO) and imperialist competitive algorithm (ICA). A comparative study between these hybrid algorithms was performed by Ebdali et al. (2020). This study, among others, showed that the performance prediction of the PSO-ANN is superior to other hybrid models. The use of a powerful optimization algorithm such as PSO improves significantly the robustness and the stability of the predictive model by avoiding local minima and converging to the true global optimal ANN parameters rapidly and accurately (Cai et al., 2020). However, the best performance of the PSO-ANN model can be achieved only if its parameters (number of particles and coefficients of velocity) have been selected adequately. Unfortunately, there is no theoretical analysis to find the optimum values of these parameters which is the biggest disadvantage of the PSO-ANN method (Han et al., 2019). For this reason, it is common to use trial and error approach or conduct sensitivity analysis in order to obtain best results.

Although the development of hybrid models in civil engineering applications remains limited, some recent studies (Akkurt et al., 2003; Qi et al., 2018; Ali Jallal et al., 2019; Boukhatem et al., 2019) were able to develop successfully ANN models combined with GA or PSO.

Our research focuses on the development of a metaheuristic model capable of predicting the compressive strength of limestone fillers RCC to be used to build dams. An experimental database of RCC formulations was taken from lab activity reports about four Algerian dams and based on this data, an ANN model and another PSO-ANN hybrid model were developed. Therefore, an experimental program on RCC in the laboratory was carried out to validate the models.

2. Optimization Method

2.1 Artificial Neural Network (ANN)

The ANN is a system inspired by the human brain functioning. This system type "black box" is able to weave relationships between the neurons that compose it in order to solve problems of optimization, prediction and classification (Dan et al., 2002). It is composed of elements named artificial neurons connected to each other by connections weighted with weights "W" and biases "b" associated with each neuron (Borne et al., 2007). In 1943, a first mathematical model was proposed to understand and mimic human brain function (Mcculloch and Pitts, 1943). Since, several types of ANN are developed (Ghaderi et al., 2019) In the present study, we considered the backpropagation multilayer perceptron (BPMLP) which is the most used in the field. The structure of the ANN is constituted of three layers: input layer, hidden layer and output layer (Siddique and Adeli, 2013). The data considered allowed to create a function between inputs and outputs by means of a learning algorithm.

Figure 1. displays the overall scheme of an ANN network functioning. The neurons of the input layer receive the data attributed for each neuron (X_1, X_2...X_i). Thereafter, the data of the input layer will be transferred to the neurons of the hidden layer by links weighted by weights (W_1, W_2 .... W_i). The state of the hidden layer neurons is determined by an activation function "f(x)"" generally chosen from the sigmoid form Eq. (1). The values of the neurons in the hidden layer will then be combined and passed in the same way to the output layer, which calculates the final result.

$$f(x) = tansing(n) = \frac{2}{(1+e^{-2n}-1)} \quad (1)$$

2.2 Particle Swarm Optimization (PSO)

The PSO is a simulation algorithm inspired by the social behaviour of different populations of animal species developed by Kennedy and Eberhart (1997). Its effectiveness proves solving

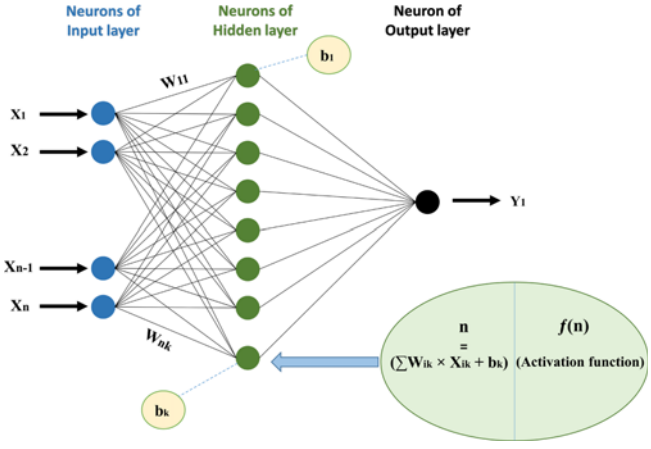

Fig. 1. Architecture of a Multilayer Perceptron Neural Network

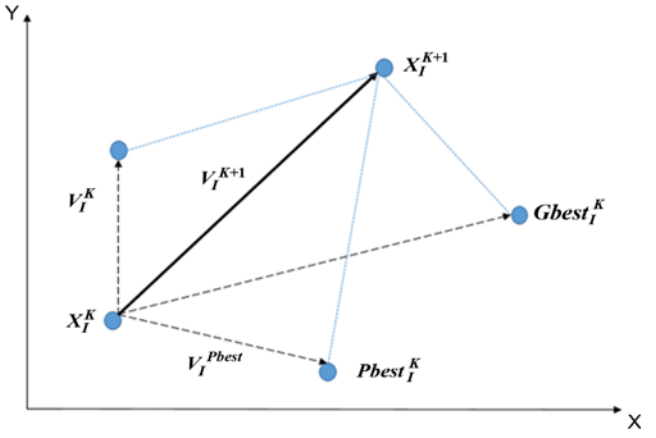

Fig. 2. Search Mechanism of Particle Swarm Optimization

global optimisation problems in several scientific fields such as in hydraulics (Patil et al., 2020), civil engineering (Perampalam et al., 2019) and ambient energy (Maleki, 2019). The operation of the PSO is described in Eqs. (2) and (3) and represented by Fig. 2:

$$V_I^{K+1} = w \times V_I^K + r_1 C_1 \times (Pbest_I^K - X_I^K) + r_2 C_2 \times (Gbest_I^K - X_I^K), \quad (2)$$

$$X_I^{K+1} = X_I^K + V_I^{K+1}, \quad (3)$$

where w is the inertia of the particle; V_I^{K+1}, V_I^K and X_I^{K+1},X_I^K represent respectively velocities (current and new) and positions (current and new); C_1 and C_2 are acceleration factors; r_1 and r_2 are arbitrary values between 0 and 1; $Pbest_I^K$ is the best location for particle I and $Gbest_I^K$ is the best location obtained by the group.

2.3 Hybrid Model (PSO-ANN)

The effectiveness of ANN is based on the optimization of the network parameters (weight and bias), done by learning algorithms that are limited in case of complex problems and make the learning process relatively slow (Rebouh et al., 2017). In order to best optimize the ANN model, a hybrid PSO-ANN system has been developed where the PSO works to optimize the weights (W) and biases (b) of the ANN.

Figure 3. explains the operation steps of the proposed model. Each set of ANN weights and biases is considered as a particle of the PSO swarm. Initially, the particles will be initialized randomly, each particle is represented by a given position Xi in the particle search domain. Then, for each new generation, the positions and velocity will be updated. According to the fitness function of the ANN, the parameters *Pbest* and *Gbest* are corrected and the final positions of the particles will be obtained by updating Eqs. (2) and (3) until the optimal values of the parameters of ANN are obtained.

3. Development of the Prediction Model

3.1 Database

The database is built from RCC formulations taken from lab

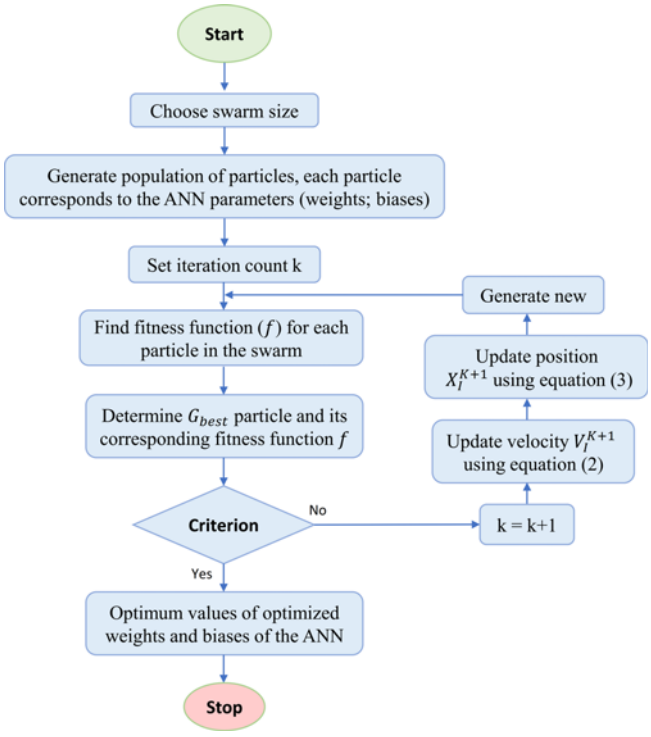

Fig. 3. Flowchart of the PSO-ANN Model

activity reports drawn up for the construction of four (04) Algerian dams: Koudiat-Acerdoun, Tabellout, Ouljet-Mellegue and Boussiaba. We were sent the data by the ANBT Algerian agency "Agence Nationale des Barrages et Transfères" which is the project owner. The reports contain information about all the RCC formulations (Characteristics of materials, rates and properties of RCC) used in the construction of the dams. According to these reports, the type of cement used is CEM II/A 42.5 with an average compressive strength of 44 MPa. The cement proposed contains 15 to 20% of limestone addition. The granular mixtures of the RCC used are made up of limestone fillers ($CaCO_3$ > 85%), coarse sand 0/5 as well as class A or B gravel according to standard NF EN 12620 (2003) (Gravel 5/20 and ballast of 20/40, 20/50 or 20/63 according to the dam project). For all granular mixtures, the proportions of the aggregates used were determined to meet the requirements of a referential particle size distribution (Fig. 4).

Of the 04 reports exploited, 600 raw data vectors were collected and after analysis, 500 vectors which proved to be richer were selected. Each vector consisted of important parameters having a direct impact on the RCC compressive strength: the maximum diameter of the aggregates (Dmax), the compactness of the dry granular mixture (C), the cement rate (Dc), the limestone filler rate (Df), the Water/Cement ratio (W/C) and the RCC age (A). Table 1 shows some examples of the collected information in

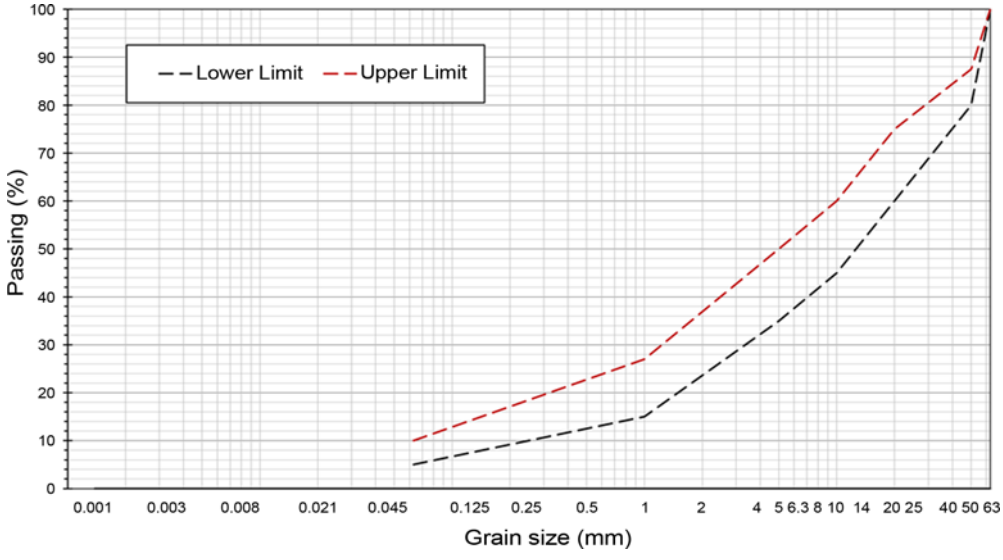

Fig. 4. Particle Size Distribution of Reference

Table 1. Examples and Limit Values of RCC Formulations from the Database

Parameters	Dmax (mm)	Compactness C	Cement rate Dc (Kg/m^3)	Filler rate Df (Kg/m^3)	W/C ratio	Age A (Day)	Compressive strength Fc (MPa)
1	40	0.84	140	133	0.75	28	15.35
2	50	0.85	110	140	1.05	90	14
3	63	0.85	120	145	0.7	28	14.4
Min. value	40	0.80	70	60	0.58	28	4.9
Max. value	63	0.90	170	170	1.14	90	24.1

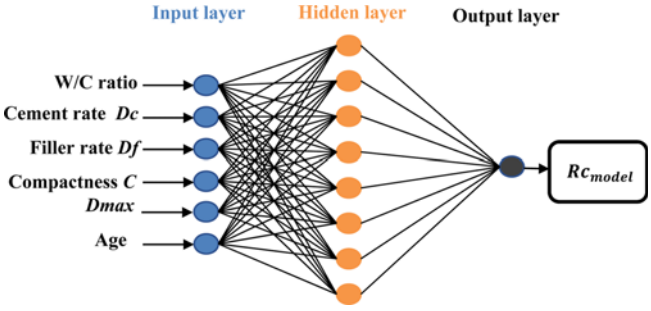

Fig. 5. Architecture of Model (ANN) of the Compressive Strength Prediction

addition to the minimal and maximal values of each parameter.

3.2 ANN and PSO-ANN Models

Based on the parameters of the RCC composition selected (Dmax, C, Dc, Df, W/C and A), the input layer composed of six neurons. The neuron of the output layer represents the RCC compressive strength "Fc model" which will be predicted. To choose the best architecture of the hidden layer, a series of simulations were carried out using the Levenberg-Marquardt learning algorithm. The database was divided into three parts: 70% for learning, 15% for testing and 15% for validation. The neural network of the highest performance has eight neurons in the hidden layer. This architecture (06 input neurons, 08 hidden neurons and 01 output neuron), represented by Fig. 5, will be taken in to consideration in the rest of our study.

In order to improve the performance of the proposed ANN, a PSO algorithm was used for learning (determination of optimal weights and biases). According to Alam et al. (2015), The PSO algorithm parameters C_1 and C_2 yield the best results when ranging from 1 to 2.5 and 2 to 3 respectively. By varying these two acceleration coefficients within the recommended ranges, the best results were achieved when the values $C_1 = 1.5$ and $C_2 = 2.5$ were applied. Thus, the different parameters of the PSO-ANN model proposed to predict the compressive strength are

Table 2. PSO-ANN Parameters Considered

ANN			PSO			
Input layer	Hidden layer	Output layer	Iteration	C_1	C_2	Swarm
6	8	1	2,000	1.5	2.5	400

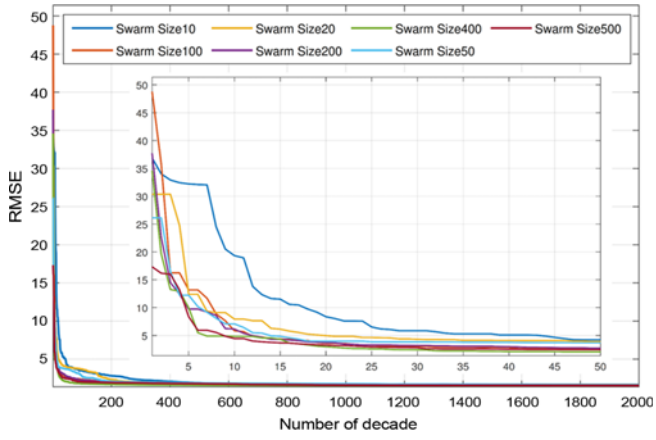

Fig. 6. Variation of the Quadratic Error as a Function of the Number of Iterations

presented in Table 2. The variation of the root mean square error "RMSE", shown in Fig. 6, is a function of the iteration number for the swarm size. The first fifty iterations were enlarged to show the influence of the swarm size PSO on the prediction error of the model. The best compressive strength prediction model was obtained when the swarm size is 400.

The regression results between the experimental values and those predicted by the ANN model and the PSO-ANN model are shown in Figs. 7 and 8, respectively. Each figure shows the regression of the 15% of the data set reserved for the test, as well as the regression of the all data.

The reliability of the proposed models was analyzed using two performance indices: the root mean square error "RMSE"

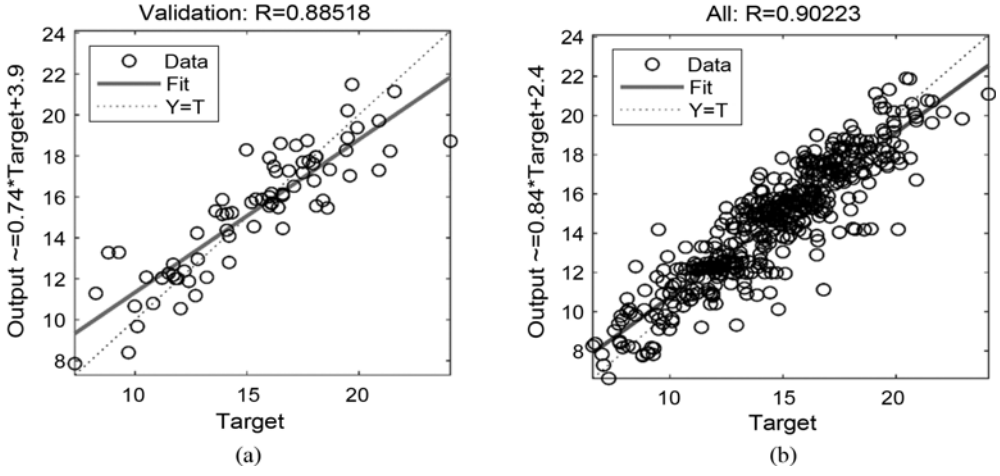

Fig. 7. Regression Results from the ANN Model: (a) Validation Data, (b) All Data

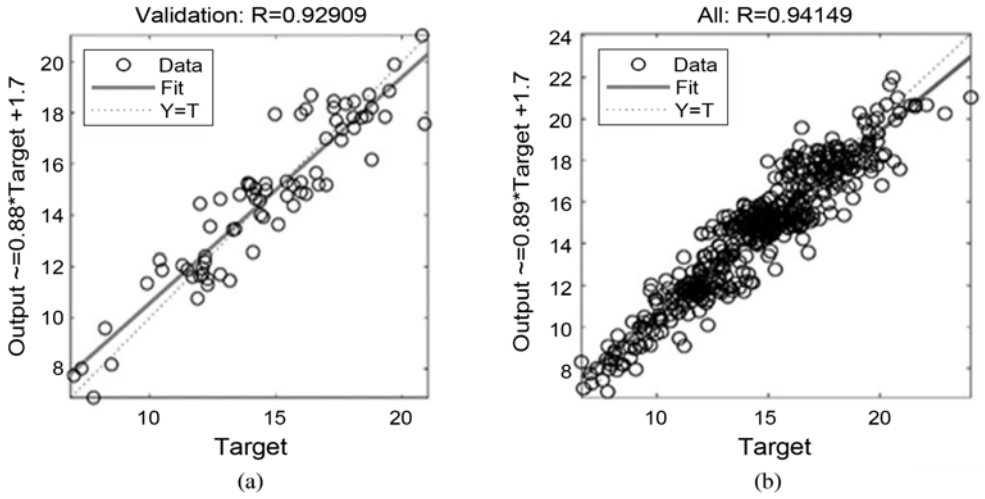

Fig. 8. Regression Results from the PSO-ANN Model: (a) Validation Data, (b) All Data

Table 3. Performance Parameters for the Models Studied

Model	RMSE	R^2
ANN	1.342	0.82
PSO-ANN	1.227	0.89

Eq. (4) and the coefficient of determination "R^2" which explains the degree of connection between the experimental values (y_i) and those predicted by the model ($\hat{y}_i$) Eq. (5). The performances of the two models proposed in this study are shown in Table 3.

$$RMSE = \sqrt{\left(\frac{1}{N}\right)\sum_i (y_i - \hat{y}_i)^2}, \tag{4}$$

$$R^2 = 1 - \left(\frac{\sum_i (y_i - \hat{y}_i)^2}{\sum_i (y_i - \bar{y})^2}\right), \tag{5}$$

where N is the number of measurements and $\bar{y}$ is the average value of these measurements.

Based on these results, parameters of the PSO-ANN model are significantly better than those of the ANN model. In fact, compared to the ANN model, the RMSE of the PSO-ANN model decreased approximately by 8.5% and its factor R^2 increased by 8.5%. The latter indicates a better efficiency of the PSO-ANN model, and therefore the efficiency of the PSO to optimize the ANN parameters (weight and bias) in comparison with the Levenberg-Marquardt algorithm has been validated. After the PSO-ANN model has proven its accuracy in predicting the RCC compressive strength compared to the ANN model, only the PSO-ANN model will be taken into account in the rest of the study.

3.3 Influence of Cement Strength

As previously discussed, the models developed (ANN and PSO-ANN) to predict the RCC compressive strength relying on six (06) input parameters (Dmax, C, Dc, Df, W/C and A), without regardless of the variation of the cement compressive strength

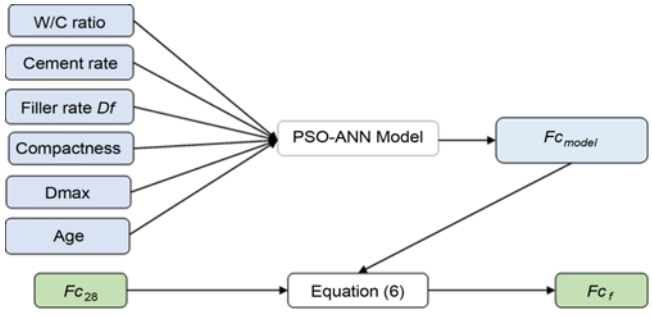

Fig. 9. Global Model for Prediction the Strength of RCC

for 28 days "Fc_{28}", which has a considerable influence on the concrete strength (Dupain et al., 2004). In fact, all methods of concrete formulation take into consideration the cement strength. The LCPC method, which is applicable to RCC, proposes a formula to predict the strength of concrete according to Fc_{28} Eq. (7), and is itself based on the Féret equation (de Larrard, 1999b). Similarly, as for conventional concrete, basically all known methods (Bolomey, Dreux Gorisse or Walz), offer similar equations (Dupain et al., 2004). All these equations indicate a linear variation between the concrete compressive strength and the cement strength, with the same concrete composition. Based on this and considering an average value of the cement strength (Fc_{28} = 44 MPa) used in the preparation of the database RCC (according to the lab activity reports), a corrective relation Eq. (6) was proposed. This equation proposes to correct the RCC compressive strength predicted by the model, if the cement strength is different to 44 MPa. Indeed, if the cement strength is equal to 44 MPa, the Eq. (6) is used without correction. This equation, which only applies in our case, is integrated into the global RCC strength prediction model, shown in Fig. 9. Therefore, the final value of the compressive strength F_{c_f} of the RCC is calculated after correcting $F_{c_{model}}$.

$$F_{c_f} = F_{c_{model}} \times \left(1 + \left(\frac{F_{c_{28}} - 44}{44}\right)\right), \tag{6}$$

with

F_{c_f} : Final compressive strength

$F_{c_{model}}$: Model predicted compressive strength.

4. Experimental Validation

4.1 Experimental Study

In order to test the efficiency of the PSO-ANN model, an experimental tests were conducted on 20 RCC formulations. As for the granular mixtures of the RCC, a limestone filler was used (0/1 mm with an 80 µm sieve pass of about 85%) whose physical and chemical properties are presented in Table 4. In addition to that, sand 0/5 mm, limestone gravel (3/8, 8/15, 15/25) and 25/40 or 25/50 ballast were used. Their main properties are described in Table 5. Proportions of the different aggregates (Table 7) were determined to obtain granular mixtures whose curves are included in the referential particle size distribution (Fig. 4). Fig. 10 shows an example of the granular mixtures used in the experiment.

Table 4. Physico-Chemical Characteristics of Limestone Fillers 0/1

Chemical characteristics			Physical characteristics		
$CaCO_3$ (%)	CaO (%)	SiO_2 (%)	Specific weight (t/m^3)	Apparent density	Refractive index
98	55.18	0.06	2.7	1.31	1.71

Table 5. Physical and Mechanical Characteristics of the Aggregates Used

Aggregate	Los angeles coefficient	Flattening coefficient	Absorption (%)	Specific gravity
Sand 0/5	-	-	0.27	2.72
Gravel 3/8	22	23	0.66	2.71
Gravel 8/15		17	0.73	2.69
Gravel 15/25		13	0.7	2.68
Ballast 25/50	21	5	-	2.69

Table 6. Chemical Composition of Cement

Composants	SiO_2	Al_2O_3	F_eO_3	CaO	MgO	SO_3
Rate (%)	17.19	4.17	3.06	62.17	1.72	2.33

A Portland cement type CEM II/42.5 is used with a compressive strength of 50.1 MPa in 28 days and a fineness of 4,156 g/cm², containing 17% limestone addition obtained from a local cement plant. Its chemical composition is presented in Table 6. Furthermore, about 1% (in cement weight) of a modified polycarboxylates-based superplasticizer is used to achieve the desired consistency of the mixtures.

The 20 formulations of RCC, which presented in Table 7, were obtained by varying the main input parameters used in the prediction model (Dmax, C, Dc, Df, and W/C). these parameters were selected to best reflect their variations in the database used. Firstly, the compactness "C" of the various dry granular mixtures were measured according to NF EN 13286-5 standard (2003) in the lab. After mixing the RCC, their consistency was measured with the VEBE test according to the ASTM C1170-91 (1998).

The VEBE time was maintained between 18 and 22s. Thus, for each formulation, six (06) cylindrical moulds 160 mm (diam.) × 320 mm were set up with compaction under mass and vibration according to ASTM C1176-92 (1998). After 24 hours, the samples were demoulded and conserved under water at a temperature of 20 ± 2°C until the testing time. After 28 and 90 days, the compressive strength were measured according to NF EN 12390-3 (2012). Fig. 13 shows some photos of the experimental tests carried-out.

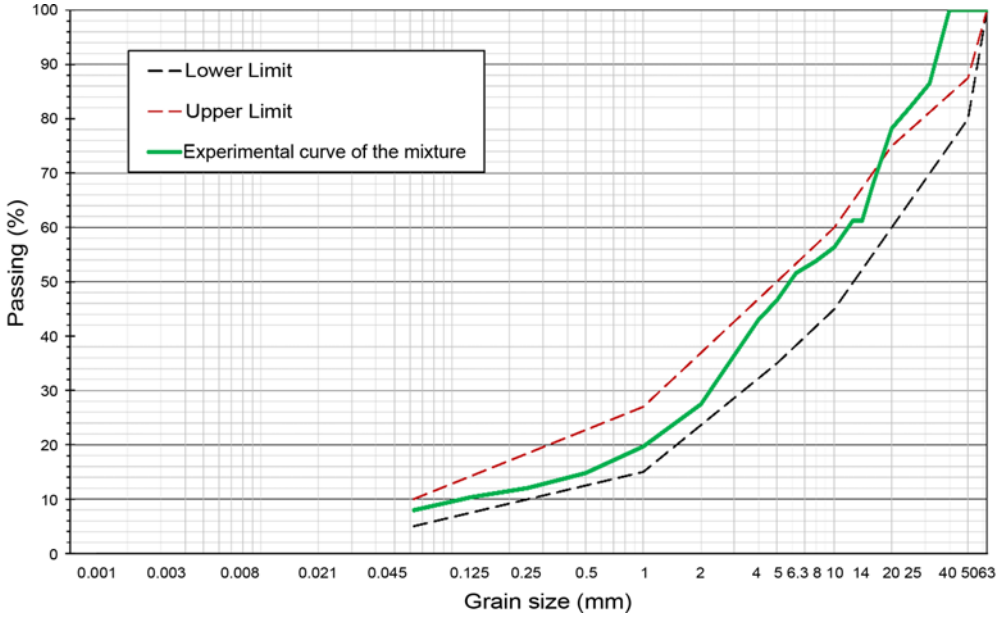

Fig. 10. Particle Size Curves of Granular Mixtures

Table 7. RCC Compositions Studied

Designation	Aggregate D max (mm)	Limestone filler (Kg/m³)	Cement (Kg/m³)	W/C ratio	Sand (Kg/m³)	Gravels (Kg/m³)	Ballast Kg/m³)
RCC(40)1	40	120.75	145	0.70	906.83	796.80	407.52
RCC(40)2		120.75	145	0.80	906.83	796.80	407.52
RCC(40)3		120.75	145	0.85	906.83	796.80	407.52
RCC(40)4		138.24	130	0.70	911.47	810.89	410.16
RCC(40)5		138.24	130	0.80	911.47	810.89	410.16
RCC(40)6		138.24	130	0.85	911.47	810.89	410.16
RCC(40)7		150.72	115	0.65	920.70	807.55	414.32
RCC(40)8		150.72	115	0.70	920.70	807.55	414.32
RCC(40)9		150.72	115	0.75	920.70	807.55	414.32
RCC(40)10		150.72	115	0.80	920.70	807.55	414.32
RCC(50)1	50	123.65	145	0.70	928.62	815.95	417.31
RCC(50)2		123.65	145	0.80	928.62	815.95	417.31
RCC(50)3		123.65	145	0.85	928.62	815.95	417.31
RCC(50)4		138.81	130	0.70	915.21	814.22	411.85
RCC(50)5		138.81	130	0.80	915.21	814.22	411.85
RCC(50)6		138.81	130	0.85	915.21	814.22	411.85
RCC(50)7		150.06	115	0.70	916.65	803.99	412.49
RCC(50)8		146.03	115	0.75	905.38	796.38	407.42
RCC(50)9		150.06	115	0.80	916.65	803.99	412.49
RCC(50)10		150.06	115	0.85	916.65	803.99	412.49

4.2 Results and Discussion

In order to validate the results of the PSO-ANN model developed to predict of the RCC compressive strength, a comparative study is carried out for this. The results of prediction obtained from the final PSO-ANN model were compared with those of the experimental validation study. On the other hand, another comparison was made between the results of the experimental study and those obtained from the method developed by LCPC (Zdiri et al., 2008). The LCPC method is based on a global empirical equation (Eq. (7)) to predict compressive strength. This equation takes into consideration several parameters such as the constant Kg, related to the granular mix used, the 28-day cement strength "Rc_{28}", the concrete age parameter d(t), the EMP factor calculated by Eq. (8) according to Dmax, g* and g (compactness parameters of the granular mix). Moreover, the global prediction equation takes into account the volume of cement Vc, the volume of water Ve and the volume of entrapped air V_a.

$$f_c(t) = K_g Rc_{28}\left[d(t)+\left(\frac{V_C}{V_C+V_e+V_a}\right)^{2,85}\right]EMP^{-0.13} \quad (7)$$

$$EMP = Dmax\left(\sqrt[3]{\frac{g^*}{g}}-1\right) \quad (8)$$

Figures 11 and 12 show a comparison of the experimental strengths with those predicted by the PSO-ANN model and the LCPC method, respectively. The performance indices R^2 and RMSE of the two correlations are presented in Table 8.

Based on Fig. 11, the LCPC method was not very accurate in predicting strength of the studied RCC. In fact, a low coefficient of determination R^2 in order of 0.47 was obtained with an RMSE of 2.70. However, the PSO-ANN model (Fig. 12), showed a significant correlation with a coefficient of determination R^2 in order of 0.85 and an RMSE value of 1.45. In comparison with the results of the LCPC method, an 80% improvement in the factor of determination as well as a 45% decrease in the root mean square error, were all observed. This fact confirms the efficiency of the PSO-ANN model. However, the strength values predicted by the PSO-ANN model are slightly underestimated compared to the experimental values. This underestimation of around 6% on average (estimated by comparing the regression

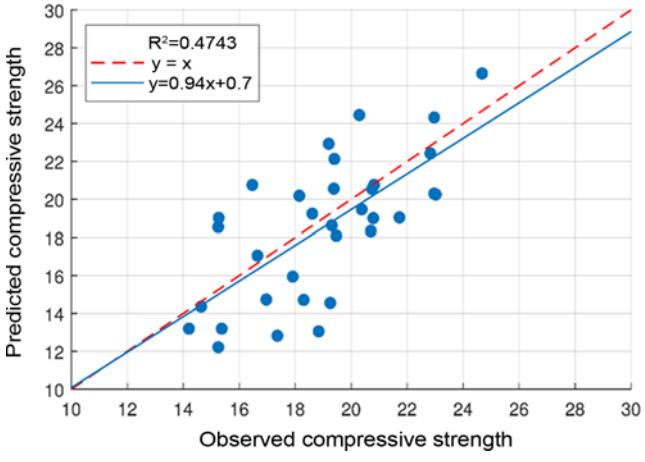

Fig. 11. Linear Regression between Experimental Results and Those Simulated by the LCPC Method

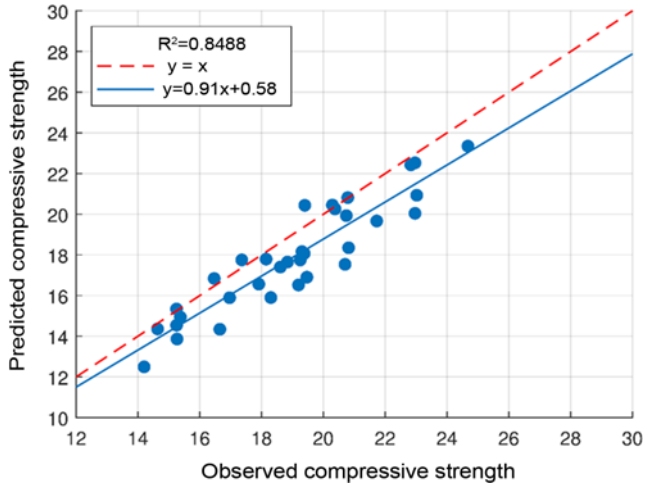

Fig. 12. Linear Regression between Experimental Results and PSO-ANN Predicted Results

Table 8. Statistical Parameters of the Regressions

Model	RMSE	R^2
ANN-PSO	1.45	0.849
LCPC	2.70	0.473

line with the line Y = X), remains nevertheless insignificant and can be explained by the few minor differences in terms of materials and implementation, which are not considered as input parameters in the model, such as the compaction mode of concrete or the type and superplasticizer dosage. Didouche et al. (2018), found a strength variation from 8.5 to 10 MPa by varying the content from 0.6 to 1.5% of two superplasticizers (melamine resin and polycarboxylate). In our case, the content of superplasticizer is not very variable but the type was not the same as the concretes in the database and those in the experimental validation study. Furthermore, the database concrete specimens were compacted using a percussion hammer according to ASTM C1435-99 (1999), whereas in our experimental study, ASTM C1176-92 (1998) was adopted where a vibrating table was used. Even if both compaction methods are normalized, they still remain different. Liu et al. (2015), noted that the implementation of concrete specimens directly influences the compressive strength. Şengün et al. (2019), demonstrated that the presence of 5% voids in concrete due to incomplete compaction could lead to a loss of strength of up to 30%.

However, the error of prediction identified by the PSO-ANN model remains minimal, especially that the method for measuring the compressive strength (according to NF EN 12390-3, 2012) itself tolerates an error value of 11.7%, under a tests reproducibility conditions.

4.3 Development of a User Interface Based on the Fc Prediction Model

In order to make the task easier for users, a visual interface based on the final prediction model was developed (Fig. 14), end done

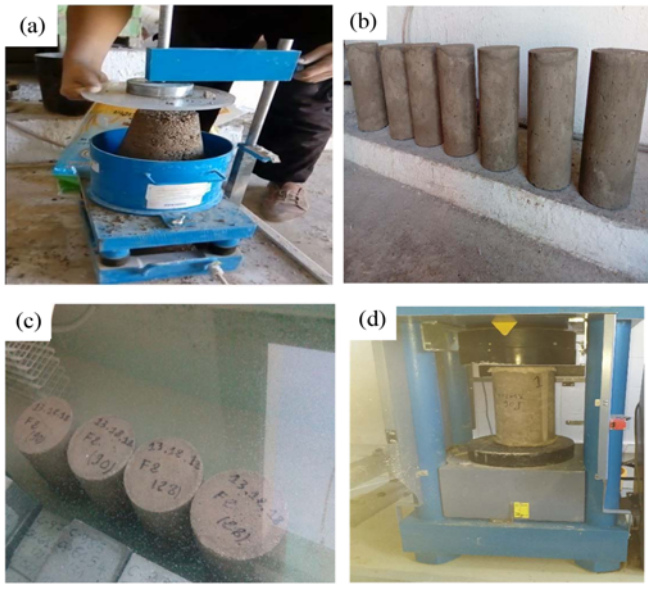

Fig. 13. Photos of the Experimental Study: (a) Verification of No Slump and Calculation of the VEBE Time, (b) RCC Specimens, (c) Conditioning of Specimens before Testing, (d) Compressive Strength Test

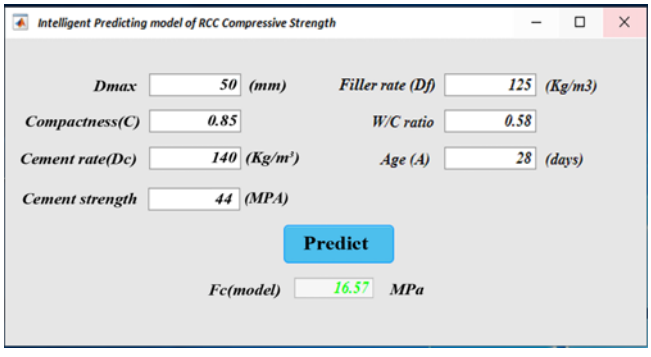

Fig. 14. PSO-ANN Interactive Graphical User Interface

using the "app designer" functionality of Matlab 2019 software. The user has to puts in the values of the different input parameters, namely: maximum diameter of aggregate (Dmax), compactness of the dry granular mix (C), cement rate (Dc) and its strength (Fc28), limestone filler rate (Df), water/cement ratio (W/C) and the age of the (RCC) (28 or 90 days). By pressing the "Calculate" button, the predicted compressive strength value is dispelled.

5. Conclusions

In this study, a hybrid intelligent prediction system was developed, combining two metaheuristics (ANN and PSO). This hybridization shows its efficiency compared to the classical ANN system optimized with a Levenberg-Marquardt algorithm. The richness of the database that was used (500 vectors) as well as the wide ranges of variations of the different formulation parameters (inputs) or strength (output), gave the system a good learning curve, and therefore more credibility.

The model was experimentally validated in the lab and compared with the LCPC method. Even with few differences in the materials and in the way the concrete was casted, the system developed (PSO-ANN) showed very good predictive capability of the RCC strength tested with a high value of the coefficient of determination ($R^2 = 0.85$). The obtained results by the LCPC method were not very accurate because of a low value of the coefficient of determination $R^2 = 0.47$.

Ultimately, through this system, an effective tool is developed to predict the compressive strength of the limestone fillers concrete that is used to build dams. Moreover, in order to make the model easy to use, a visual user-friendly interface was set up.

Acknowledgments

Not Applicable

ORCID

Not Applicable

References

ACI Committee 207 (1999) Roller-compacted mass concrete. ACI 207.5R-99, American Concrete Institute, Farmington Hills, MI, USA

ACI Committee 209 (2008) Guide for modelling and calculating shrinkage and creep in hardened concrete. ACI 209.2R-08, American Concrete Institute, Farmington Hills, MI, USA

Akkurt S, Ozdemir S, Tayfur G, Akyol B (2003) The use of GA–ANNs in the modelling of compressive strength of cement mortar. *Cement and Concrete Research* 33(7):973-979, DOI: 10.1016/S0008-8846(03)00006-1

Alam MN, Das B, Pant V (2015) A comparative study of metaheuristic optimization approaches for directional overcurrent relays coordination. *Electric Power Systems Research* 128:39-52, DOI: 10.1016/j.epsr.2015.06.018

Ali Jallal M, Chabaa S, Zeroual A (2019) A novel deep neural network based on randomly occurring distributed delayed PSO algorithm for monitoring the energy produced by four dual-axis solar trackers. *Renewable Energy* 149:1182-1196, DOI: 10.1016/j.renene.2019.10.117

Amlashi AT, Abdollahi SM, Goodarzi S, Ghanizadeh AR (2019) Soft computing based formulations for slump, compressive strength, and elastic modulus of bentonite plastic concrete. *Journal of Cleaner Production* 230:1197-1216, DOI: 10.1016/j.jclepro.2019.05.168

ASTM C1170-91 (1998) Standard test methods for determining consistency and density of roller-compacted concrete using a vibrating table. ASTM C1170-91, ASTM International, West Conshohocken, PA, USA

ASTM C1176-92 (1998) Standard practice for making roller-compacted concrete in cylinder molds using a vibrating table. ASTM C1176-92, ASTM International, West Conshohocken, PA, USA

ASTM C1435-99 (1999) Standard practice for molding roller-compacted concrete in cylinder molds using a vibrating hammer. ASTM C1435-99, ASTM International, West Conshohocken, PA, USA

Bai J, Wild S, Ware JA, Sabir BB (2003) Using neural networks to predict workability of concrete incorporating metakaolin and fly ash. *Advances in Engineering Software* 34(11-12):663-669, DOI: 10.1016/S0965-9978(03)00102-9

Belić M, Bobić V, Badža M, Šolaja N, Đurić-Jovičić M, Kostić VS (2019) Artificial intelligence for assisting diagnostics and assessment of parkinson's disease — A review. *Clinical Neurology and Neurosurgery* 184:105442, DOI: 10.1016/j.clineuro.2019.105442

Borne P, Benrajeb M, Haggège J (2007) Les réseaux de neurones présentation et applications. Editions TECHNIP, Paris, France

Boukhatem B, Rebouh R, Zidol A, Chekired M, Tagnit-Hamou A (2019) An intelligent hybrid system for predicting the tortuosity of the pore system of fly ash concrete. *Construction and Building Materials* 205:274-284, DOI: 10.1016/j.conbuildmat.2019.02.005

Boussaid I (2014) Perfectionnement de métaheuristiques pour l'optimisation continue. Paris-Est Créteil, Créteil, France, 169

Cai H, Liao T, Ren S, Li S, Huo R, Yuan J, Yang W (2020) Predicting the compressive strength of desert sand concrete using ANN: PSO and its application in tunnel. *Advances in Civil Engineering* 2020:1-11, DOI: 10.1155/2020/8875922

Calis G, Yıldızel SA (2019) Investigation of roller compacted concrete: Literature review. *Challenge Journal of Concrete Research Letters* 10(3):63, DOI: 10.20528/cjcrl.2019.03.003

Caré S, Linder R, Baroghel-Bouny V, de Larrard F, Charonnat Y (2000) Effet des additions minérales sur les propriétés d'usage des bétons Plan d'expérience et analyse statique. Institut Français des Sciences et Techniques des Réseaux, de l'Aménagement et des Transports Ed., Paris, France

Chhorn C, Hong SJ, Lee SW (2018) Relationship between compressive and tensile strengths of roller-compacted concrete. *Journal of Traffic and Transportation Engineering (English Edition)* 5(3):215-223, DOI: 10.1016/j.jtte.2017.09.002

Cyr M, Lawrence P, Ringot E (2006) Efficiency of mineral admixtures in mortars: Quantification of the physical and chemical effects of fine admixtures in relation with compressive strength. *Cement and Concrete Research* 36(2):264-277, DOI: 10.1016/j.cemconres.2005.07.001

Dan A, Oosterbaan J, Jamet P (2002) Contribution des réseaux de neurones artificiels (RNA) à la caractérisation des pollutions de sol. Exemples des pollutions en hydrocarbures aromatiques polycycliques (HAP). *Comptes Rendus Geoscience* 334(13):957-965, DOI: 10.1016/S1631-0713(02)01836-9

de Larrard F (1999a) Concrete mixture proportioning: A scientific approach. E & FN Spon, London, UK

de Larrard F (1999b) Structures granulaires et formulation des bétons. Laboratoires des Ponts et Chaussées, Paris, France

de Larrard F, Sedran T (2009) Le logiciel BétonlabPro 3. Bulletin des Laboratoires des Ponts et Chaussées, Paris, France

Didouche Z, Ezziane K, Kadri E-H (2018) Predicted of hydration heat and compressive strength of limestone cement mortar with different type of superplasticizer. *Advances in Concrete Construction* 6(6):659-677, DOI: 10.12989/ACC.2018.6.6.659

Dupain R, Lanchon R, Saint-Arroman J (2004) Granulat, sols, ciments et betons. Casteilla, Paris, France

Ebdali M, Khorasani E, Salehin S (2020) A comparative study of various hybrid neural networks and regression analysis to predict unconfined compressive strength of travertine. *Innovative Infrastructure Solutions* 5(3):93, DOI: 10.1007/s41062-020-00346-3

Elsheikh AH, Sharshir SW, Abd Elaziz M, Kabeel AE, Guilan W, Haiou Z (2019) Modeling of solar energy systems using artificial neural network: A comprehensive review. *Solar Energy* 180:622-639, DOI: 10.1016/j.solener.2019.01.037

Gauthier P, Marchand J (2004) Conception et réalisation de revêtements en béton compacté au rouleau au Québec. Association des Constructeurs

de Routes et Grands Travaux du Québec, Québec, Canada
Ghaderi A, Abbaszadeh Shahri A, Larsson S (2019) An artificial neural network based model to predict spatial soil type distribution using piezocone penetration test data (CPTu). *Bulletin of Engineering Geology and the Environment* 78(6):4579-4588, DOI: 10.1007/s10064-018-1400-9
Godoi WC, Coraiola G, Junior SR, Swinka-Filho V, de Geus K, Portella, KF, Medeiros BL, Cunha de Andrade F, Hönnicke MG (2019) Expounding structures of roller compacted concrete dam specimens by means of hard conventional X-ray inspection. *Heliyon* 5(4): e01467, DOI: 10.1016/j.heliyon.2019.e01467
Gopalakrishnan K (2013) Particle swarm optimization in civil infrastructure systems. Metaheuristic Applications in Structures and Infrastructures, Elsevier, Amsterdam, Netherlands, 49-76
Hammoudi A, Moussaceb K, Belebchouche C, Dahmoune F (2019) Comparison of artificial neural network (ANN) and response surface methodology (RSM) prediction in compressive strength of recycled concrete aggregates. *Construction and Building Materials* 209:425-436, DOI: 10.1016/j.conbuildmat.2019.03.119
Han I-J, Yuan T-F, Lee J-Y, Yoon Y-S, Kim J-H (2019) Learned prediction of compressive strength of GGBFS concrete using hybrid artificial neural network models. *Materials* 12(22):3708, DOI: 10.3390/ma12223708
International Federation for Structural Concrete (2010) Model code 2010. Comité Euro-International du Béton, Lausanne, Switzerland
Kennedy J, Eberhart RC (1997) A discrete binary version of the particle swarm algorithm. *Proceedings of the IEEE International Conference on Systems, Man and Cybernetics* 5:4104-4108, DOI: 10.1109/icsmc.1997.637339
Kitouni S, Houari H (2013) Lightweight concrete with Algerian limestone dust: Part I: Study on 30% replacement to normal aggregate at early age. *Cerâmica* 59(352):600-608, DOI: 10.1590/S0366-69132013000400017
Liu D, Li Z, Liu J (2015) Experimental study on real-time control of roller compacted concrete dam compaction quality using unit compaction energy indices. *Construction and Building Materials* 96:567-575, DOI: 10.1016/j.conbuildmat.2015.08.048
Maleki A (2019) Optimal operation of a grid-connected fuel cell based combined heat and power systems using particle swarm optimisation for residential sector. *International Journal of Ambient Energy* 42:550-557, DOI: 10.1080/01430750.2018.1562968
McCulloch W, Pitts W (1943) A logical calculus of the ideas immanent in nervous activity. *The Bulletin of Mathematical Biophysics* (5):116-133
Michel F, Piérard J, Courard L, Pollet V (2007) Influence of physico-chemical characteristics of limestone fillers on fresh and hardened mortar performances. RILEM Publications S.A.R.L
Momeni E, Jahed Armaghani D, Hajihassani M, Mohd Amin MF (2015) Prediction of uniaxial compressive strength of rock samples using hybrid particle swarm optimization-based artificial neural networks. *Measurement* 60:50-63, DOI: 10.1016/j.measurement.2014.09.075
NF EN 12620 (2003) Granulats pour béton. Association Française de Normalisation (AFNOR), France
NF EN 12390-3 (2012) Essais pour béton durci - Partie 3 : résistance à la compression des éprouvettes. Association Française de Normalisation (AFNOR), France
NF EN 13286-5 (2003) Mélanges traités et mélanges non traités aux liants hydrauliques. Association Française de Normalisation (AFNOR), France
Park K-B, Noguchi T, Plawsky J (2005) Modeling of hydration reactions using neural networks to predict the average properties of cement paste. *Cement and Concrete Research* 35(9):1676-1684, DOI: 10.1016/j.cemconres.2004.08.004
Patil MB, Naidu MN, Vasan A, Varma MRR (2020) Water distribution system design using multi-objective particle swarm optimisation. *Sādhanā* 45(1), DOI: 10.1007/s12046-019-1258-y
Perampalam G, Poologanathan K, Gunalan S, Ye J, Nagaratnam B (2019) Optimum design of cold-formed steel beams: Particle swarm optimisation and numerical analysis. *ce/papers* 3(3-4):205-210, DOI: 10.1002/cepa.1159
Qi C, Fourie A, Chen Q (2018) Neural network and particle swarm optimization for predicting the unconfined compressive strength of cemented paste backfill. *Construction and Building Materials* 159:473-478, DOI: 10.1016/j.conbuildmat.2017.11.006
Rahmani E, Sharbatdar MK, Beygi MHA (2020a) The effect of water-to-cement ratio on the fracture behaviors and ductility of Roller compacted concrete pavement (RCCP). *Theoretical and Applied Fracture Mechanics* 109:102753, DOI: 10.1016/j.tafmec.2020.102753
Rahmani E, Sharbatdar M, Kazem HA, Beygi MHA (2020b) A comprehensive investigation into the effect of water to cement ratios and cement contents on the physical and mechanical properties of roller compacted concrete pavement (RCCP). *Construction and Building Materials* 253:119177, DOI: 10.1016/j.conbuildmat.2020.119177
Rebouh R, Boukhatem B, Ghrici M, Tagnit-Hamou A (2017) A practical hybrid NNGA system for predicting the compressive strength of concrete containing natural pozzolan using an evolutionary structure. *Construction and Building Materials* 149:778-789, DOI: 10.1016/j.conbuildmat.2017.05.165
Sankar MR, Saxena S, Banik SR, Iqbal IM, Nath R, Bora LJ, Gajrani KK (2019) Experimental study and artificial neural network modeling of machining with minimum quantity cutting fluid. *Materials Today: Proceedings* 18:4921-4931, DOI: 10.1016/j.matpr.2019.07.484
Şengün E, Alam B, Shabani R, Yaman IO (2019) The effects of compaction methods and mix parameters on the properties of roller compacted concrete mixtures. *Construction and Building Materials* 228:116807, DOI: 10.1016/j.conbuildmat.2019.116807
Siddique NH, Adeli H (2013) Computational intelligence: Synergies of fuzzy logic, neural networks, and evolutionary computing. John Wiley & Sons, Hoboken, NJ, USA
Sukontasukkul P, Chaisakulkiet U, Jamsawang P, Horpibulsuk S, Jaturapitakkul C, Chindaprasirt P (2019) Case investigation on application of steel fibers in roller compacted concrete pavement in Thailand. *Case Studies in Construction Materials* 11:e00271, DOI: 10.1016/j.cscm.2019.e00271
Tan ZX, Thambiratnam DP, Chan THT, Gordan M, Abdul Razak H (2019) Damage detection in steel-concrete composite bridge using vibration characteristics and artificial neural network. *Structure and Infrastructure Engineering* 16(9):1247-1261, DOI: 10.1080/15732479.2019. 1696378
Yeh I-C (2006) Exploring concrete slump model using artificial neural networks. *Journal of Computing in Civil Engineering* 20(3):217-221, DOI: 10.1061/(ASCE)0887-3801(2006)20:3(217)
Yildizel SA, Calis G, Tayeh BA (2020) Mechanical and durability properties of ground calcium carbonate-added roller-compacted concrete for pavement. *Journal of Materials Research and Technology* 9(6):13341-13351, DOI: 10.1016/j.jmrt.2020.09.070
Zdiri M, Ben Ouezdou M, Neji J (2008) Theoretical and experimental study of roller-compacted concrete strength. *Magazine of Concrete Research* 60(7):469-474, DOI: 10.1680/macr.2007.00002
Zhang P, Gao Z, Shi Y, Lin Y, Li J (2020) Effect of large broken stone content on properties of roller compacted concrete based on fractal theory. *Construction and Building Materials* 262:120821, DOI: 10.1016/j.conbuildmat.2020.120821